


## TRANSLATIONAL SCIENCE

# Immune response to dermatomyositis-specific autoantigen, transcriptional intermediary factor 1 $\gamma$ can result in experimental myositis

Naoko Okiyama ,<sup>1</sup> Yuki Ichimura,<sup>1</sup> Miwako Shobo,<sup>1</sup> Ryota Tanaka,<sup>1</sup> Noriko Kubota,<sup>1</sup> Akimasa Saito,<sup>1</sup> Yosuke Ishitsuka,<sup>1,2</sup> Rei Watanabe,<sup>1,2</sup> Yasuhiro Fujisawa,<sup>1</sup> Yoshiyuki Nakamura,<sup>1</sup> Akihiro Murakami,<sup>3</sup> Hisako Kayama,<sup>4</sup> Kiyoshi Takeda,<sup>5</sup> Manabu Fujimoto<sup>1,6</sup>

**Handling editor** Josef S Smolen

► Additional supplemental material is published online only. To view, please visit the journal online (<http://dx.doi.org/10.1136/annrheumdis-2020-218661>).

For numbered affiliations see end of article.

## Correspondence to

Dr Naoko Okiyama, Department of Dermatology, Faculty of Medicine, University of Tsukuba, Tsukuba 305-8575, Japan; [naoko.okiyama@md.tsukuba.ac.jp](mailto:naoko.okiyama@md.tsukuba.ac.jp)

Received 21 July 2020

Revised 9 March 2021

Accepted 21 March 2021

## ABSTRACT

**Objectives** To investigate whether autoimmunity to transcriptional intermediary factor 1 (TIF1) $\gamma$ , a ubiquitous nuclear autoantigen for myositis-specific autoantibodies detected in patients with dermatomyositis (DM) is pathogenetic for inflammatory myopathy.

**Methods** Wild-type,  $\beta_2$ -microglobulin-null, perforin-null, I $\gamma$  $\mu$ -null and interferon  $\alpha/\beta$  receptor (IFNAR)-null mice were immunised with recombinant human TIF1 $\gamma$  whole protein. A thymidine incorporation assay was performed using lymph node T cells from TIF1 $\gamma$ -immunised mice. Plasma was analysed using immunoprecipitation followed by western blot analysis and enzyme-linked immunosorbent assays. Femoral muscles were histologically and immunohistochemically evaluated. CD8<sup>+</sup> or CD4<sup>+</sup> T cells isolated from lymph node T cells or IgG purified from plasma were adoptively transferred to naïve mice. TIF1 $\gamma$ -immunised mice were treated with anti-CD8 depleting antibody and a Janus kinase inhibitor, tofacitinib.

**Results** Immunisation with TIF1 $\gamma$ -induced experimental myositis presenting with necrosis/atrophy of muscle fibres accompanied by CD8<sup>+</sup> T cell infiltration successfully in wild-type mice, in which TIF1 $\gamma$ -specific T cells and antihuman and murine TIF1 $\gamma$  IgG antibodies were detected. The incidence and severity of myositis were significantly lower in  $\beta_2$ -microglobulin-null, perforin-null, CD8-depleted or IFNAR-null mice, while I $\gamma$  $\mu$ -null mice developed myositis normally. Adoptive transfer of CD8<sup>+</sup> T cells induced myositis in recipients, while transfer of CD4<sup>+</sup> T cells or IgG did not. Treatment with tofacitinib inhibited TIF1 $\gamma$ -induced myositis.

**Conclusions** Here we show that TIF1 $\gamma$  is immunogenic enough to cause experimental myositis, in which CD8<sup>+</sup> T cells and type I interferons, but not CD4<sup>+</sup> T cells, B cells or antibodies, are required. This murine model would be a tool for understanding the pathologies of DM.

## INTRODUCTION

Idiopathic inflammatory myopathies (IIMs) include dermatomyositis (DM), polymyositis, immune-mediated necrotising myopathy (IMNM), inclusion body myositis and antisynthetase syndrome (ASS), characterised by inflammation of muscles and other organs.<sup>1,2</sup> Autoimmunity mediates these diseases, as a number of myositis-specific autoantibodies have been identified<sup>3–6</sup> and are associated with distinct

## Key messages

### What is already known about this subject?

- A number of autoantibodies have been identified in sera of patients with dermatomyositis (DM), which are not only highly disease specific but are associated with distinct clinical features.
- One of the autoantigens for the myositis-specific autoantibodies, transcriptional intermediary factor 1 (TIF1) $\gamma$ , is a ubiquitous intracellular molecule that is often mutated or overexpressed in tumours and triggers the development of anti-TIF1 $\gamma$  antibody-positive DM.
- Previously established murine models of experimental autoimmune myositis are dependent on immune responses against muscle tissue-specific antigens.

### What does this study add?

- Autoimmunity against TIF1 $\gamma$  results in experimental myositis.
- The initiation of the experimental myositis is completely dependent on autoreactive TIF1 $\gamma$ -specific CD8<sup>+</sup> T cells, but not on CD4<sup>+</sup> T cells or IgG.
- The type I interferon pathway is partially involved in the pathogenesis of myositis caused by autoimmunity against TIF1 $\gamma$ .

### How might this impact on clinical practice or future developments?

- Autoimmunity to TIF1 $\gamma$  is not only a diagnostic marker for a subset of human DM and may play a role in the pathogenesis of the DM seen in patients with these autoantibodies.
- This new murine model of experimental myositis might be a useful tool to investigate pathologic mechanisms of, and to develop specific treatments for, human anti-TIF1 $\gamma$  antibody-positive DM.

clinical features.<sup>7</sup> In DM, five autoantibodies have been identified: anti-Mi-2, antimelanoma differentiation-associated gene 5, antitranscriptional intermediary factor 1 (TIF1),<sup>8,9</sup> antinuclear



© Author(s) (or their employer(s)) 2021. No commercial re-use. See rights and permissions. Published by BMJ.

**To cite:** Okiyama N, Ichimura Y, Shobo M, et al. *Ann Rheum Dis* Epub ahead of print: [please include Day Month Year]. doi:10.1136/annrheumdis-2020-218661

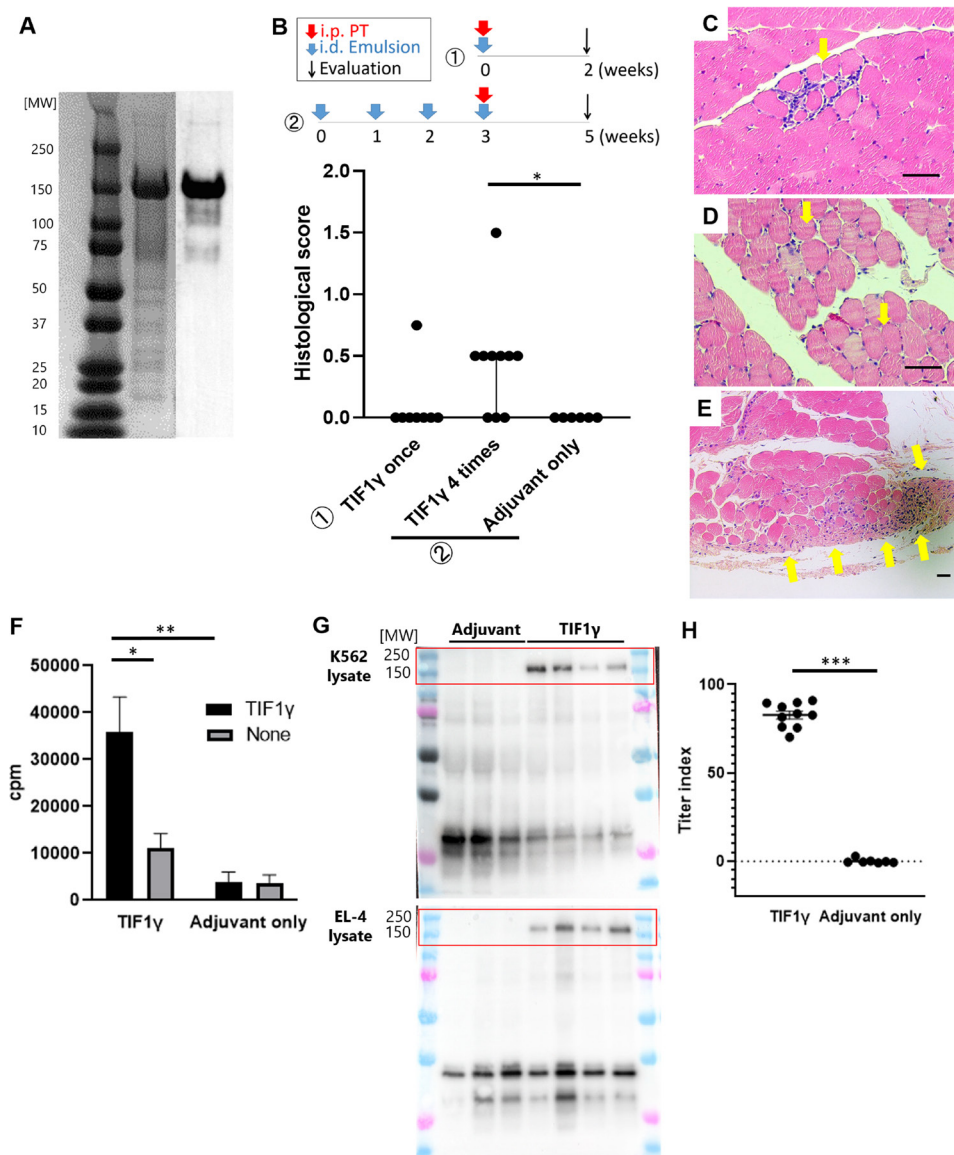


**Figure 1** Development of experimental myositis dependent on the immune response to transcriptional intermediary factor 1 (TIF1) $\gamma$ . (A) Sodium dodecyl sulphate-polyacrylamide gel electrophoresis (second lane) followed by a western blotting assay using anti-TIF1 $\gamma$  antibodies (third lane) revealed that the purified protein has a molecular weight (MW) of about 150 kDa, which is consistent with TIF1 $\gamma$  whole protein. MW markers are shown in first lane. (B) The upper panel shows our immunisation protocols. Mice received intraperitoneal injection (i.p.) of pertussis toxin (PT), and intradermal injection of an emulsion of complete Freund's adjuvant with/without TIF1 $\gamma$  protein at the back and foot pads. The graph shows histological scores for experimental myositis in the hamstrings and quadriceps of mice immunised once (n=8) and four times (n=10) with TIF1 $\gamma$  whole protein, and mice immunised with adjuvant only four times (n=6). Dots and bars represent individuals and medians with interquartile ranges (IRs), respectively. \*p<0.05 by Kruskal-Wallis test with Dunn's multiple comparisons test. (C–E) Representative myositis (yellow arrows) with muscle fibre atrophy (C) or necrosis (D), and perifascicular atrophy (E) observed in H&E-stained sections of muscle tissues from TIF1 $\gamma$ -immunised mice. Bars represent 50  $\mu$ m. (F)  $^3$ H thymidine incorporation (cpm) in T cells from regional lymph nodes of TIF1 $\gamma$ -immunised mice (n=3) co-cultured with bone marrow-derived dendritic cells (BMDCs) presenting TIF1 $\gamma$ . T cells from mice immunised BMDCs pulsed with adjuvant only (n=3) or without antigen were used as control T cells and control BMDCs, respectively. Bars represent means with SE of the mean (SEM). \*p<0.05, and \*\*p<0.01 by two-way ANOVA with Tukey's multiple comparisons test. (G) IgGs binding TIF1 $\gamma$  antigens from K562 and EL-4 cell lysates, the MWs of which were between 150 and 250 kDa, were detected in the plasma of TIF1 $\gamma$ -immunised mice (n=4), but not in plasma from mice immunised with adjuvant only (n=3). (H) Enzyme-linked immunosorbent assay conducted with plasma from TIF1 $\gamma$ -immunised mice (n=10) and mice immunised with adjuvant only (n=7). The titre index calculation method is detailed in online supplemental materials and methods. Dots and bars represent individuals and means with SEM, respectively. \*\*\*p<0.001 by Student's t-test. Data are representative of two independent experiments.

matrix protein 2 and antismall ubiquitin-like modifier activating enzyme.

While autoantibodies against various nuclear/cytoplasmic components serve as diagnostic tools for systemic autoimmune diseases, a direct causative role for most of them has been questioned. TIF1 $\gamma$ , a major antigen of anti-TIF1 antibodies,

is a 155 kDa nuclear protein belonging to the tripartite motif superfamily.<sup>8,9</sup> Anti-TIF1 $\gamma$  antibody is present in a quarter of adult/juvenile patients with DM<sup>10,11</sup> and is associated with an increased risk of malignancies in elderly patients.<sup>12–14</sup> TIF1 $\gamma$  was found to be overexpressed not only in tumours<sup>15</sup> but also in muscle tissues, especially in regenerating atrophic perifascicular

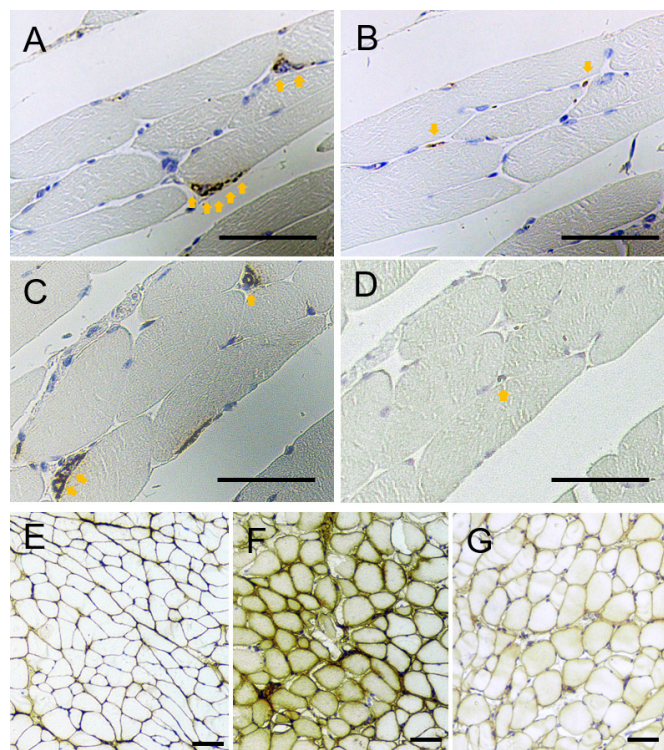


**Figure 2** Infiltration of inflammatory cells and upregulation of major histocompatibility complex (MHC) class I molecules in muscle tissues. (A–D) Immunohistochemical (IHC) analyses of CD8 (A), CD4 (B), CD11b (C) and B220 (D) on the mononuclear cells infiltrating into the endomysium areas of the muscle tissues of TIF1 $\gamma$ -immunised mice. (E–G) IHC analyses of MHC class I molecules on the cell membranes of the muscle fibres in control adjuvant-treated mice (E) and in TIF1 $\gamma$ -immunised mice (F), compared with the isotype-control antibody-stained samples from TIF1 $\gamma$ -immunised mice (G) Data are representative of three independent experiments.

myofibers and in skin.<sup>16 17</sup> Our observations revealed that pregnancy might trigger the development of anti-TIF1 $\gamma$  antibody-positive DM,<sup>18</sup> which would be related to overexpression of TIF1 $\gamma$  antigen in the embryo and mammary epithelial cells during pregnancy.<sup>19 20</sup> While this evidence suggests the aetiologic roles of TIF1 $\gamma$ , it remains unknown whether autoimmunity to TIF1 $\gamma$  is directly involved in disease pathogenesis. Here we show that experimental myositis can develop following immunisation with recombinant TIF1 $\gamma$  protein.

## METHODS

### Mice

Female C57BL/6 (B6) mice 8–10 weeks of age were purchased from Charles River. Beta<sub>2</sub>-microglobulin ( $\beta_2$ MG)-null, perforin-null and Ig $\mu$ -null ( $\mu$ MT) B6 mice and interferon  $\alpha/\beta$  receptor (IFNAR)-null B6 mice<sup>21</sup> were purchased from The Jackson Laboratory and B&K Universal. All experiments were carried out under specific pathogen-free conditions in accordance with the University of Tsukuba's ethics and safety guidelines for animal experiments.

### Recombinant human TIF1 $\gamma$ protein

A full-length human TIF1 $\gamma$  gene (GenBank accession number: AF119043) was His-tagged at its 3' end and inserted into pFastBac1 vector for baculovirus expression (invitrogen). The detailed protocol for the expression and purification of

recombinant TIF1 $\gamma$  protein is described in online supplemental materials and methods. Human TIF1 $\gamma$  whole protein is 93.3% homologous with the murine protein.

### Induction of experimental myositis

Mice were immunised intradermally with 200  $\mu$ g of TIF1 $\gamma$  protein emulsified in complete Freund's adjuvant (CFA) containing 100  $\mu$ g of heat-killed *Mycobacterium butyricum* (Difco) once in the back and in foot pads along with an intraperitoneal injection of 250 ng of pertussis toxin (PT, Wako Junyaku). Other mice were immunised intradermally with the CFA emulsion containing TIF1 $\gamma$  protein four times weekly at multiple sites of the back and foot pads. The same time as the last (fourth) intradermal injection of the emulsion, 250 ng of PT was once injected intraperitoneally. Mice treated with CFA (weekly, 4 times) and PT were used as controls. These immunisation protocols are presented in [figure 1B](#). Following the evaluation method for C protein-induced myositis (CIM),<sup>22</sup> three H&E-stained sections from the hamstring and quadriceps each were blinded to the intervention and examined histologically for necrosis/atrophy of muscle fibres accompanied by mononuclear cell infiltration. The scoring system is detailed in online supplemental materials and methods.

### Sodium dodecyl sulphate-polyacrylamide gel electrophoresis and western blotting assay and immunoprecipitation followed by western blot assay

Fifty microliters of mouse plasma were combined with 50  $\mu$ L of Protein G Sepharose 4 Fast Flow (GE Healthcare) for 2 hours at room temperature. Antibody-bound sepharose beads were washed with immunoprecipitation (IPP) buffer (10 mM tris-HCl, pH 8.0; 50 mM NaCl and 0.1% 4-nonylphenyl-polyethylene glycol (BioVision)) and incubated with extracts from  $1 \times 10^7$  K562 human cells and EL-4 murine cells (American Type Culture Collection (ATCC)), respectively, for 2 hours at 4°C. Purified recombinant TIF1 $\gamma$  protein, K562-precipitated protein and EL-4-precipitated protein were fractionated by sodium dodecyl sulphate-polyacrylamide gel electrophoresis (SDS-PAGE) using

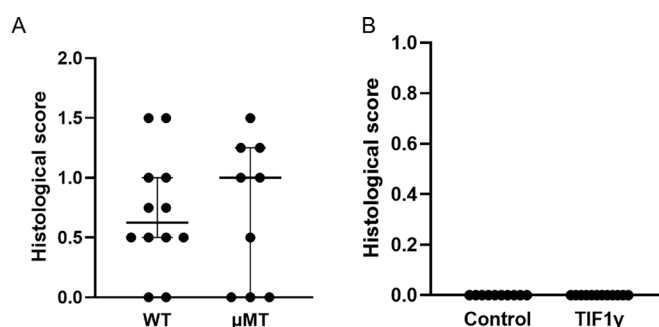


**Figure 3** TIF1 $\gamma$ -specific B cell linages and antibodies are not required for the development of TIF1 $\gamma$ -induced myositis. (A) Histologic scores for experimental myositis in hamstrings and quadriceps of  $\mu$ MT mice immunised with TIF1 $\gamma$  whole protein (n=9) were equal to TIF1 $\gamma$ -immunised wild-type (WT) mice (n=12). Dots and bars represent individuals and medians with IRs, respectively. (B) Histologic scores for experimental myositis in the hamstrings and quadriceps of recipient mice (n=12) with adoptive intravenous transfer of IgGs purified from pooled plasma of TIF1 $\gamma$ -immunised mice or control recipients (n=10) of IgGs from pooled plasma of mice immunised with adjuvant only. Dots and bars represent individuals and medians with IRs, respectively. Data are representative of two independent experiments. IRs, interquartile ranges.

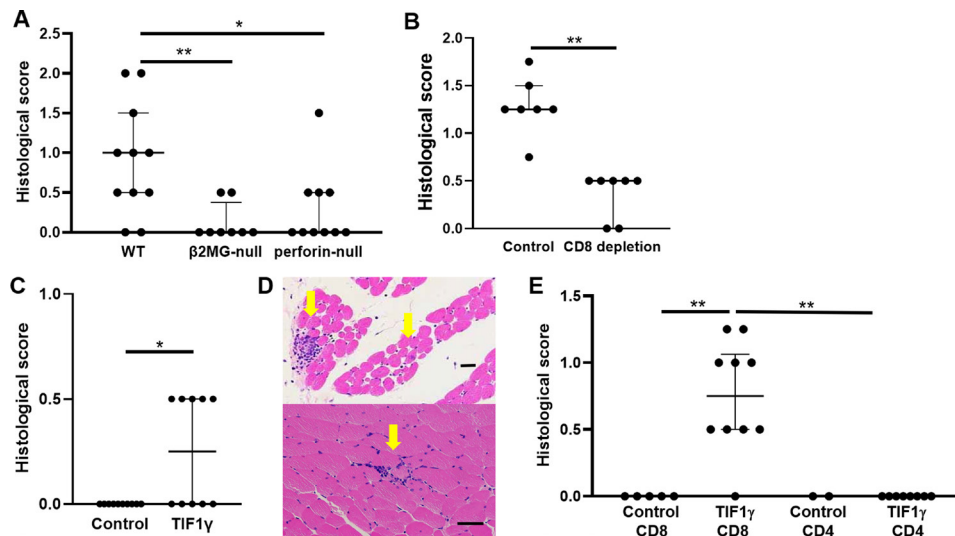


**Figure 4** TIF1 $\gamma$ -specific CD8<sup>+</sup> T cells are critical for the development of TIF1 $\gamma$ -induced myositis. (A) Histological scores for experimental myositis in the hamstrings and quadriceps of WT mice (n=11),  $\beta_2$ -microglobulin ( $\beta_2$ MG)-null mice (n=8), and perforin-null mice (n=10) 2 weeks after fourth immunisation with TIF1 $\gamma$  whole protein. Dots and bars represent individuals and medians with IRs, respectively. \* $p$ <0.05, and \*\* $p$ <0.01 by Kruskal-Wallis test with Dunn's multiple comparisons test. (B) Histological scores for experimental myositis of TIF1 $\gamma$ -immunised mice treated with anti-CD8 depleting antibody (n=7) compared with those treated with control antibody (n=7). Dots and bars represent individuals and medians with IRs, respectively. \*\* $p$ <0.01 by Mann-Whitney  $U$  test. (C) Histological scores for experimental myositis in the hamstrings and quadriceps of recipient mice (n=10) following adoptive intravenous transfer of TIF1 $\gamma$ -activated T cells originally purified from pooled lymph node cells of TIF1 $\gamma$ -immunised mice compared with TIF1 $\gamma$ -activated T cells originally from pooled lymph node cells of mice immunised with adjuvant only (n=10). Dots and bars represent individuals and medians with IRs, respectively. \* $p$ <0.05 by Mann-Whitney  $U$  test. (D) Representative myositis (yellow arrows) in HE-stained sections of muscle tissues from TIF1 $\gamma$ -specific T cell-recipients. Bars represent 50  $\mu$ m. (E) Histological scores for experimental myositis in hamstrings and quadriceps of TIF1 $\gamma$ -CD8 recipient mice (n=10) following adoptive intravenous transfer of CD8<sup>+</sup> T cells purified from TIF1 $\gamma$ -specific T cells compared with transfer of TIF1 $\gamma$ -CD4 recipient mice (n=8) with adoptive intravenous transfer of CD4<sup>+</sup> T cells purified from TIF1 $\gamma$ -specific T cells and control CD8 recipients (n=5) following adoptive intravenous transfer of CD8<sup>+</sup> T cells purified from T cells of mice immunised with adjuvant only. Lack of myositis in control CD4 recipients (n=2) following adoptive intravenous transfer of CD4<sup>+</sup> T cells purified from T cells of mice immunised with adjuvant only. Dots and bars represent individuals and medians with IRs, respectively. \*\* $p$ <0.01 by Kruskal-Wallis test with Dunn's multiple comparisons test. Data are representative of two independent experiments. IRs, interquartile ranges.

10% polyacrylamide gels, applied to Mini-PROTEANTGX precast gels (4%–15%, Bio-Rad Laboratories). The gel on which recombinant TIF1 $\gamma$  protein was applied was stained with Bio-Safe Coomassie Stain (Bio-Rad Laboratories). For western blotting (WB) assay, proteins were transferred onto nitrocellulose membranes using a wet transfer apparatus (Mini Trans-Blot Cell, Bio-Rad Laboratories) from the gels. The membranes were blocked with 5% skim milk and incubated with rabbit antihuman/murine TIF1 $\gamma$  polyclonal antibody (NB100-57498, Novus Biologicals), antihuman TIF1 $\gamma$  polyclonal antibodies (LS-C408048, LifeSpan Biosciences) and antimurine TIF1 $\gamma$  polyclonal antibodies (ab47062; Abcam), respectively, overnight at 4°C. They were washed with tris-buffered saline with Tween 20, incubated with peroxidase-labelled goat antirabbit IgG polyclonal antibodies (sc-2004, Santa Cruz Biotechnology) and then visualised using SuperSignal West Pico (Thermo Fisher Scientific).

#### Enzyme-linked immunosorbent assay

The plasma samples collected from immunised mice 2 weeks after the last immunisation were evaluated in our established enzyme-linked immunosorbent assay (ELISA) system (online supplemental materials and methods).

#### Immunohistochemical analyses

CD8, CD4, CD11b and B220-positive cells and upregulation of H-2Kb molecules were detected on sections from muscle tissue samples (online supplemental materials and methods).

#### In vivo depletion of CD8<sup>+</sup> T cells

To deplete CD8<sup>+</sup> T cells, mice were intraperitoneally injected with purified rat anti-CD8 $\alpha$  depleting monoclonal antibody (53.67.2) in the protocol as shown previously<sup>22</sup> and as described in online supplemental materials and methods.

#### Adoptive transfer of T cells or IgG

T cells were purified from the inguinal and popliteal lymph node (LN) cells of immunised mice 2 weeks after the fourth immunisation using CD3 T cell enrichment columns (R&D systems). Three million T cells were cultured with  $1.5 \times 10^5$  TIF1 $\gamma$ -pulsed mature bone marrow-derived dendritic cells (BMDCs, generated in the protocol shown in online supplemental materials) and 100 U/mL recombinant murine IL-2 (PeproTec) in 2 mL RPMI1640 with 10% fetal bovine serum (FBS) for 72 hours using 24-well culture plates. CD8-positive or CD4-positive T cells were sorted with MACS magnetic beads (Miltenyi Biotech). Flow cytometric analyses showed that the purities of the sorted CD8<sup>+</sup> and CD4<sup>+</sup> T cells were >95%, and that CD11c-positive DCs were absent. IgG was purified from the plasma of immunised mice 2 weeks after the fourth immunisation using protein G columns (Ab-Rapid SPiN Ex, ProteNova). One million whole T cells,  $4 \times 10^5$  CD8-positive or CD4-positive T cells or 500  $\mu$ g of IgG were intravenously injected into recipient mice that had been pretreated with CFA.<sup>23</sup> The muscles of the hind legs were evaluated histologically 2 weeks after transfer.

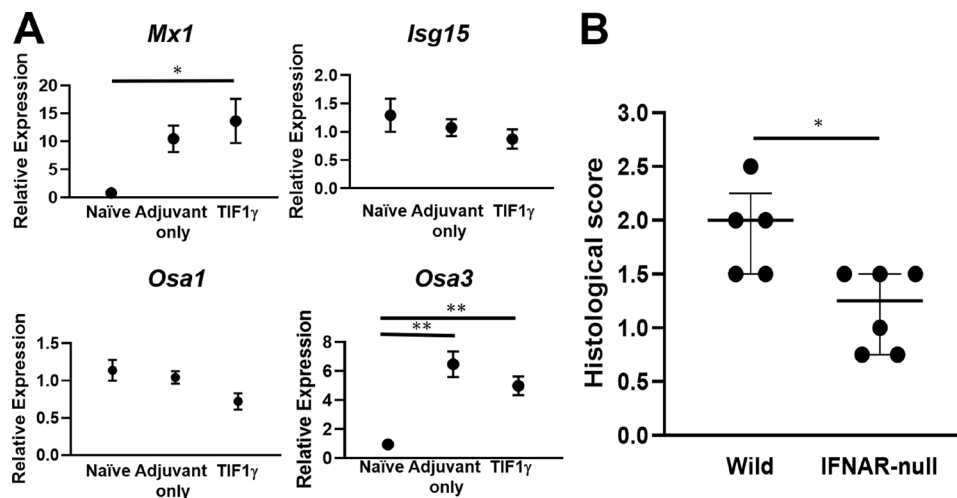


**Figure 5** Type I interferon (IFN) signalling in the pathogenesis of TIF1 $\gamma$ -induced myositis. (A) Fold changes in mRNA levels of type I IFN-related genes, *Mx1*, *Isg15*, *Osa1* and *Osa3*, which were normalised against  $\beta$ -actin mRNA levels, in muscle tissues from naive, adjuvant-treated, and TIF1 $\gamma$ -immunised mice 2 weeks after fourth immunisation.  $n=2-6$  in each group. Bars represent the means with SEMs. \* $p<0.05$ , and \*\* $p<0.01$  by ordinary one-way analysis of variance. (B) Histological scores for experimental myositis in the hamstrings and quadriceps of wild-type ( $n=5$ ) and IFN  $\alpha/\beta$  receptor-null mice ( $n=6$ ) 2 weeks after the fourth TIF1 $\gamma$  immunisation. Dots and bars represent individuals and the medians with IQRs, respectively. \* $p<0.05$  by Mann-Whitney  $U$  test.

### Real-time quantitative polymerase chain reaction analyses

As shown in online supplemental materials and methods and online supplemental table 1), real-time quantitative polymerase chain reaction (RT-qPCR) analyses were performed on total RNA extracted from the muscle tissue samples.

### Treatment with the Janus kinase inhibitor tofacitinib

In accordance with a previous report,<sup>24</sup> tofacitinib (MedChemExpress) in 0.5% methylcellulose/0.025% Tween 20 was orally administered to mice at 12.5 or 50 mg/kg Twice daily from the day of fourth immunisation of TIF1 $\gamma$ .

### Statistical analysis

Data were analysed with Prism 8 (GraphPad Software).  $P$  values less than 0.05 were considered significant.

## RESULTS

### TIF1 $\gamma$ -immunised mice develop experimental myositis

SDS-PAGE and WB revealed that the purified recombinant human whole TIF1 $\gamma$  protein contained few contaminants (figure 1A). Wild-type (WT) B6 mice immunised with the TIF1 $\gamma$  protein four times weekly developed myositis 2 weeks after the fourth immunisations in their hamstrings and quadriceps as assessed histologically. The incidence rate and the median (IQRs) of histologic scores were 70% and 0.5 (0–0.5), while none of the mice treated only with adjuvant was affected ( $p=0.0143$ ; figure 1B). The mice immunised once with TIF1 $\gamma$  rarely did (12.5% and 0 [0–0]; figure 1B) as well as the mice treated only with adjuvant ( $p>0.9999$ ). No mice exhibited significant weight loss during the observation period. Histologic analysis of muscles from the mice immunised with TIF1 $\gamma$  four times showed atrophy and necrosis of muscle fibres accompanied by infiltrating mononuclear cells in the perifascicular and endomysial sites of the muscle tissue (figure 1C,D), sometimes (in one per five samples) typical perifascicular atrophy (figure 1E). Myositis was still observed in 60% of the immunised mice 3 weeks after the fourth immunisation (incidence rate, 60%; median (IQRs) of histologic score,

0.500 (0–1.250);  $n=5$ ), and some mice also presented myositis 1 week later (60%, 0.500 (0–0.625);  $n=5$ ). No inflammation was observed in other organs, including skin, cardiac muscles and lungs.

Thymidine incorporation assay was performed as shown in online supplemental materials and methods. T cells from mice with TIF1 $\gamma$ -induced myositis (TIM) proliferated significantly more than T cells from control mice treated only with adjuvants when cocultured with TIF1 $\gamma$ -presenting BMDCs (the means $\pm$ SEMs of <sup>3</sup>H thymidine incorporation were  $35899\pm 7411$  and  $3940\pm 2086$  (cpm), respectively;  $p=0.0022$ ). T cells from TIM or control mice did not proliferate when cocultured with BMDCs presenting no specific antigen ( $11055\pm 3156$  and  $3600\pm 1782$  (cpm), respectively,  $p=0.6218$ ; figure 1F). IPP-WB analysis demonstrated the existence of not only antihuman TIF1 $\gamma$  antibodies reacting to the human cell (K562) lysate but also antimurine TIF1 $\gamma$  autoantibodies reacting to the murine cell (EL-4) lysate in the plasma from TIM mice, but not in that from CFA-treated control mice (figure 1G). Our ELISA system demonstrated higher titers of anti-TIF1 $\gamma$  antibodies in TIM mice (the mean $\pm$ SEM of titre index was  $82.8\pm 2.2$ ) compared with control mice ( $0.1\pm 0.5$ ,  $p=0.0005$ ; figure 1H).

### CD8<sup>+</sup> T cells predominantly adhere to muscle fibres, which upregulate major histocompatibility complex class I molecules, in the muscle tissues of TIM mice

Immunohistochemical analyses of the muscle tissues of TIM mice revealed that CD8<sup>+</sup> cells predominantly infiltrated into the endomysium areas and adhered to the muscle fibres (figure 2A). On the other hand, only a few CD4<sup>+</sup> cells (figure 2B), CD11b<sup>+</sup> macrophages (figure 2C), and B220<sup>+</sup> B cells (figure 2D) infiltrated into the endomysium areas. Moreover, major histocompatibility complex (MHC) class I molecules were upregulated on the cell membranes of the muscle fibres in TIM mice (figure 2F) compared with those in control adjuvant-treated mice (figure 2E) and the isotype-control antibody-stained TIM samples (figure 2G).

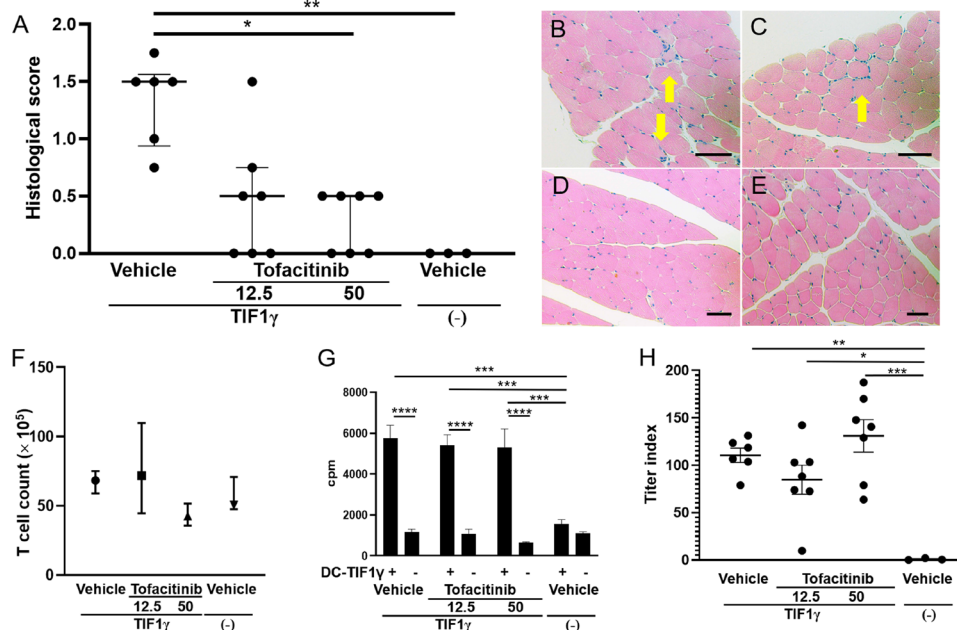


**Figure 6** Inhibitory effect of tofacitinib on TIF1 $\gamma$ -induced myositis. (A) Histological scores for experimental myositis in the hamstrings and quadriceps of TIF1 $\gamma$ -immunised mice treated with low dose (12.5 mg/kg, two times per day; n=7) or high dose (50 mg/kg, two times per day; n=7) tofacitinib from the fourth day of TIF1 $\gamma$  immunisation compared with control vehicle-treated TIF1 $\gamma$ -immunised mice (n=6) and control vehicle-treated mice immunised with adjuvant alone. Dots and bars represent individuals and medians with IRs, respectively. \* $p$ <0.05, and \*\* $p$ <0.01 by Kruskal-Wallis test with Dunn's multiple comparisons test. (B–E) Representative H&E-stained sections of muscle tissues from TIF1 $\gamma$ -immunised mice treated with control vehicle (B) low-dose tofacitinib, (C) high-dose tofacitinib and (D) control vehicle-treated mice immunised without any antigens (E). Yellow arrows show myositis and bars represent 50  $\mu$ m. (F) Total T cells in the regional lymph nodes per mouse. TIF1 $\gamma$ -immunised treated vehicle control (n=5), low-dose tofacitinib (n=5) and high-dose tofacitinib (n=5), and vehicle control-treated mice immunised without any antigens (n=3), were counted after T cell purification. Dots/squares/triangles and bars represent medians and interquartile ranges, respectively. (G) Proliferation of purified T cells from TIF1 $\gamma$ -immunised mice treated with vehicle, low-dose tofacitinib, and high-dose tofacitinib compared with those from control vehicle-treated mice immunised without any antigens when co-cultured with bone marrow-derived dendritic cells presenting TIF1 $\gamma$  (DC-TIF1 $\gamma$ ) or with dendritic cells lacking antigen. Bars represent means with SEMs. \*\*\* $p$ <0.001, and \*\*\*\* $p$ <0.0001 by two-way analysis of variance (ANOVA) with Tukey's multiple comparisons test. (H) ELISA of plasma from TIF1 $\gamma$ -immunised mice treated with control vehicle, low-dose tofacitinib, or high-dose tofacitinib (n=6–7, each) compared with mice immunised with adjuvant alone (n=3). Dots and bars represent individuals and means with SEMs, respectively. \*\* $p$ <0.05, \* $p$ <0.01, and \*\*\* $p$ <0.0001 by ordinary one-way ANOVA.

### TIF1 $\gamma$ -specific B cell lineages and antibodies are not required for the initiation of TIM

$\mu$ MT mice, which completely lack B cell lineages, developed myositis (the incidence and the median $\pm$ IQR of histologic scores were 67% and 1.000 (0–1.250)) at a similar incidence and severity as observed in WT mice (83% and 0.625 (0.500–1.000),  $p$ =0.9014) when immunised with TIF1 $\gamma$  emulsion (figure 3A). Moreover, intravenous adoptive transfer of the IgG purified from pooled plasma of TIM mice did not induce myositis in recipient mice (figure 3B).

**TIF1 $\gamma$ -specific CD8<sup>+</sup> T cells are involved in the initiation of TIM**  
 $\beta_2$ MG-null mice lacking MHC class I expression and perforin-null mice rarely developed TIM (figure 4A). While the incidence rate and the median histologic score with IQRs for TIM were 82% and 1.000 (0.500–1.500) in WT mice, they were 29% and 0 (0–0.375) in  $\beta_2$ MG-null and 40% and 0 (0–0.500) in perforin-null mice ( $p$ =0.0054 and  $p$ =0.0123 vs WT mice, respectively). Mice treated with anti-CD8 depleting antibody rarely presented TIM (the incidence rate and the median histologic score with IQRs, 71.4% and 0.500 (0–0.500)) compared with control mice (100% and 1.250 (1.250–1.500),  $p$ =0.0006; figure 4B).

Moreover, adoptive transfer of enriched TIF1 $\gamma$ -specific T cells derived from TIM mice-induced TIM-like myositis with an incidence of 50% in naïve recipient mice (the median (IQRs) of

histologic scores was 0.250 (0–0.500)), while transfer of CFA-treated mouse-derived T cells stimulated by TIF1 $\gamma$ -presenting BMDCs did not ( $p$ =0.0325, figure 4C,D). Adoptive transfer of CD8<sup>+</sup> T cells from TIM mice-induced myositis with a high incidence (90%) as well as muscle damage (the median (IRs) of histologic scores was 0.750 (0.500–1.063)); however, transfer of CD4<sup>+</sup> T cells from TIM mice did not ( $p$ =0.0010) nor did CD8<sup>+</sup> T cells from CFA-treated control mice ( $p$ =0.0067, figure 4E).

### Type I interferon partially mediates the pathogenesis of TIM

Our RT-qPCR analyses revealed that the mRNA expression of type I interferon (IFN)-related genes, *Mx1* and *Osa3*, was significantly upregulated in the muscle tissues of the TIM mice (the mean $\pm$ SEM, 11.3 $\pm$ 4.49 and 3.66 $\pm$ 0.11) compared with those of naïve mice (0.86 $\pm$ 0.14 and 0.95 $\pm$ 0.11;  $p$ =0.0205 and 0.0063, respectively); however, *Osa3* mRNA expression was also upregulated in adjuvant-treated control mice (5.96 $\pm$ 1.00,  $p$ =0.0019 vs naïve mice, figure 5A). Upregulation of mRNA expression for other type I IFN-related genes, *Isg15* and *Oas1*, was not observed in the muscle tissues of TIM mice or control mice (figure 5A). IFNAR-null mice developed milder myositis (the medians (IQRs) of the histological scores, 1.250 (0.750–1.500)) than WT mice after TIF1 $\gamma$  immunisations (2.000 (2.250–1.500),  $p$ =0.0433, figure 5B).

### Treatment with a JAK inhibitor, tofacitinib, inhibits the development of TIM

TIF1 $\gamma$ -immunised mice treated with high dose (50 mg/kg, two times per day) or low dose (12.5 mg/kg, two times per day) of tofacitinib starting on the fourth day of TIF1 $\gamma$  immunisation developed milder myositis (the medians (IQRs) of histologic scores were 0.500 (0–0.500) and 0.500 (0–0.7500), respectively) at a lower incidence rate (57% and 57%, respectively) than vehicle control-treated mice (1.500 (0.938–1.563);  $p=0.0075$  and  $0.0873$ , respectively; 100% incidence; [figure](#)). T cell counts in regional LNs of mice treated with low/high-dose tofacitinib did not differ from those of vehicle-treated mice (the medians (IRs) of T cell counts were 72 [45 – 110] and 43 [36 – 52] vs 68 [59 – 75] [ $\times 10^5$ ],  $p>0.9999$  and  $p=0.0909$ , [figure 6F](#)). Moreover, there was no inhibition of ex vivo proliferation of T cells purified from regional LNs of tofacitinib-treated TIF1 $\gamma$ -immunised mice when cocultured with TIF1 $\gamma$ -presenting BMDCs ([figure 6G](#)). This effect was significant when compared with that of mice immunised with adjuvant alone ( $p=0.0002$ ,  $0.0007$  and  $0.0009$  for TIF1 $\gamma$ -immunised mice treated with vehicle, low-dose and high-dose tofacitinib, respectively). Index values of TIF1 $\gamma$ -specific antibodies in low-dose and high-dose tofacitinib-treated TIF1 $\gamma$ -immunised mice (the means $\pm$ SEMs were  $84.7\pm 15.3$  and  $131.0\pm 17.1$ , respectively) were also equal to those in vehicle-treated TIF1 $\gamma$ -immunised mice ( $110.5\pm 7.6$ ;  $p=0.3713$  and  $0.3713$ , respectively; [figure 6H](#)).

### DISCUSSION

Our findings indicate that immunity to TIF1 $\gamma$  can contribute to the development of myositis in mice. This is the first study to demonstrate the immune response to a DM-specific autoantigen that can induce myositis. Therefore, this new experimental murine model, which we termed TIM, closely mimics human pathogenesis, especially in the initiation phase.

A number of animal models for IIMs have been established, including infectious, genetic and antigen-induced models.<sup>25–26</sup> While experimental autoimmune myositis<sup>27–28</sup> and CIM<sup>22–29</sup> completely depend on immune responses specific to muscular antigens, myosin and C protein, TIM is induced via autoimmunity generated in response to a ubiquitous intracellular molecule, which has been identified as an autoantigen in humans suffering DM. In addition to a previous report showing that muscle and lung inflammation could be induced by immunisation with purified epitopic peptides derived from conspecific histidyl-tRNA synthetase (Jo-1) as a murine model for ASS,<sup>30</sup> our results indicate that experimental myositis can be induced by immunisation with the DM-specific autoantigen. In our TIM model, mice immunised by xenogeneic (human) TIF1 $\gamma$  protein developed autoimmunity to conspecific TIF1 $\gamma$  resulting in experimental myositis, which might be due to epitope spreading to a counterpart conspecific molecule as shown in experimental autoimmune encephalomyelitis.<sup>31</sup>

TIM is initiated by cytotoxic CD8<sup>+</sup> T cells, which evokes infiltration of CD8<sup>+</sup> T cells and MHC class I upregulation in muscle fibres of patients with IIM.<sup>32–36</sup> While it has also been proven that genetically modified mice with overexpression of MHC class I in muscle tissues naturally develop myositis via endoplasmic reticulum (ER) stress,<sup>34–37</sup> our experiments showed that adoptive transfer of TIF1 $\gamma$ -specific CD8<sup>+</sup> T cells, but not of TIF1 $\gamma$ -specific CD4<sup>+</sup> T cells, caused myositis in recipient mice. This suggests that autoaggressive CD8<sup>+</sup> T cells are indicative of the development of myositis.

In contrast, B cells and autoantibodies themselves are not required for the development of TIM. Previous clinical reports indicated that the titres of anti-TIF1 $\gamma$  antibody were related to the conditions of DM<sup>38</sup> and/or the presence of internal malignancies.<sup>39–40</sup> Our findings indicate that while the immune response against TIF1 $\gamma$  is likely to mediate the induction of myositis, the development of anti-TIF1 $\gamma$  autoantibodies may be an epiphenomenon lacking direct pathogenic roles. In contrast, transfer of human IgGs from patients with IMNM, which contained antisignal recognition particle or anti-3-hydroxy-3-methylglutaryl-CoA reductase antibodies, corroborated the idea that complement can provoke muscle deficiency in recipient mice.<sup>41</sup> The difference between our experiments and this study may clarify the differences in pathogenesis of DM and IMNM.

Immunohistochemistry and gene-expression analyses of muscle and skin biopsy samples revealed that type I IFN expression correlates with DM pathogenesis.<sup>42–43</sup> Janus kinase (JAK)1 mediates downstream effects of type I IFN, and it has been reported that ruxolitinib, a JAK1/2 inhibitor, is effective for the treatment of DM case, some of which were positive for anti-TIF1 $\gamma$  antibody.<sup>44–46</sup> In addition, a report presented that treatment with tofacitinib, a JAK1/3 inhibitor, also improved myositis in a case of anti-TIF1 $\gamma$  antibody-positive DM.<sup>47</sup> Our experiments revealed that deficiency of IFNAR partially inhibits the development of TIM. Treatment of myositis with tofacitinib after the initiation of immunity to TIF1 $\gamma$  was effective; however, it did not result in significant inhibitory effects on the TIF1 $\gamma$ -specific T cells and antibodies. The mechanism underlying these results could be that the activation of type I IFN pathway induces myotube atrophy and impairs endothelial cells angiogenesis.<sup>45</sup>

Collectively, the limitations of this murine model include the lack of several DM-like phenomenons (specific rash, define muscle weakness with persistent myositis and upregulation of some type I INF-related genes in the muscle) and predominant infiltration of CD8 T cells to muscle fibres, which is not usually observed in patients with DM. Nevertheless, our new model based on autoimmunity against the ubiquitous intercellular antigen, TIF1 $\gamma$ , provides a useful tool to investigate the pathologic mechanisms of anti-TIF1 $\gamma$  antibody-positive DM.

### Author affiliations

<sup>1</sup>Department of Dermatology, Faculty of Medicine, University of Tsukuba, Tsukuba, Ibaraki, Japan

<sup>2</sup>Department of Integrative Medicine for Allergic and Immunological Disease, Graduate School of Medicine, Osaka University, Suita, Osaka, Japan

<sup>3</sup>Medical and Biological Laboratories Co Ltd, Nagoya, Aichi, Japan

<sup>4</sup>Institute for Advanced Co-Creation Studies, Osaka University, Suita, Osaka, Japan

<sup>5</sup>Department of Microbiology and Immunology, Graduate School of Medicine, Osaka University, Suita, Osaka, Japan

<sup>6</sup>Department of Dermatology, Graduate School of Medicine, Osaka University, Suita, Osaka, Japan

**Acknowledgements** Parts of this work were presented at the 3rd Global Conference on Myositis, 2019.

**Contributors** Study concept and design: NO and MF. Acquisition and analysis and interpretation of data: all authors. Drafting of the manuscript: NO and MF. Critical revision of the manuscript for important intellectual content: NO and YI. Obtained funding: NO and MF.

**Funding** Supported by KAKENHI from the Japan Society for the Promotion of Science (JSPS, 18K08263 for Naoko Okiyama).

**Competing interests** None declared.

**Patient consent for publication** Not required.

**Ethics approval** All animal studies were approved by the Institutional Animal Care and Use Committee of University of Tsukuba. This study did not involve human participants.

**Provenance and peer review** Not commissioned; externally peer reviewed.

**Data availability statement** All data relevant to the study are included in the article or uploaded as supplementary information.

**Supplemental material** This content has been supplied by the author(s). It has not been vetted by BMJ Publishing Group Limited (BMJ) and may not have been peer-reviewed. Any opinions or recommendations discussed are solely those of the author(s) and are not endorsed by BMJ. BMJ disclaims all liability and responsibility arising from any reliance placed on the content. Where the content includes any translated material, BMJ does not warrant the accuracy and reliability of the translations (including but not limited to local regulations, clinical guidelines, terminology, drug names and drug dosages), and is not responsible for any error and/or omissions arising from translation and adaptation or otherwise.

#### ORCID iD

Naoko Okiyama <http://orcid.org/0000-0002-5398-0773>

#### REFERENCES

- Schmidt J. Current classification and management of inflammatory myopathies. *J Neuromuscul Dis* 2018;5:109–29.
- Selva-O'Callaghan A, Pinal-Fernandez I, Trallero-Araguás E, et al. Classification and management of adult inflammatory myopathies. *Lancet Neurol* 2018;17:816–28.
- Lundberg LE, de Visser M, Werth VP. Classification of myositis. *Nat Rev Rheumatol* 2018;14:269–78.
- Benveniste O, Goebel H-H, Stenzel W. Biomarkers in inflammatory Myopathies-An expanded definition. *Front Neurol* 2019;10:554.
- McHugh NJ, Tansley SL. Autoantibodies in myositis. *Nat Rev Rheumatol* 2018;14:290–302.
- Mammen AL, Casciola-Rosen L, Christopher-Stine L, et al. Myositis-specific autoantibodies are specific for myositis compared to genetic muscle disease. *Neurol Neuroimmunol Neuroinflamm* 2015;2:e172.
- Okiyama N, Fujimoto M. Cutaneous manifestations of dermatomyositis characterized by myositis-specific autoantibodies. *F1000Res* 2019;8. doi:10.12688/f1000research.20646.1. [Epub ahead of print: 21 Nov 2019].
- Targoff IN, Mamurova G, Trieu EP, et al. A novel autoantibody to a 155-kd protein is associated with dermatomyositis. *Arthritis Rheum* 2006;54:3682–9.
- Kaji K, Fujimoto M, Hasegawa M, et al. Identification of a novel autoantibody reactive with 155 and 140 kDa nuclear proteins in patients with dermatomyositis: an association with malignancy. *Rheumatology* 2007;46:25–8.
- Betteridge Z, Tansley S, Shaddick G, et al. Frequency, mutual exclusivity and clinical associations of myositis autoantibodies in a combined European cohort of idiopathic inflammatory myopathy patients. *J Autoimmun* 2019;101:48–55.
- Hamaguchi Y, Kuwana M, Hoshino K, et al. Clinical correlations with dermatomyositis-specific autoantibodies in adult Japanese patients with dermatomyositis: a multicenter cross-sectional study. *Arch Dermatol* 2011;147:391–8.
- Fujimoto M, Hamaguchi Y, Kaji K, et al. Myositis-specific anti-155/140 autoantibodies target transcription intermediary factor 1 family proteins. *Arthritis Rheum* 2012;64:513–22.
- Fiorentino DF, Chung LS, Christopher-Stine L, et al. Most patients with cancer-associated dermatomyositis have antibodies to nuclear matrix protein NXP-2 or transcription intermediary factor 1 $\gamma$ . *Arthritis Rheum* 2013;65:2954–62.
- Venalis P, Selickaja S, Lundberg K, et al. Association of Anti-Transcription intermediary factor 1 $\gamma$  antibodies with paraneoplastic rheumatic syndromes other than dermatomyositis. *Arthritis Care Res* 2018;70:648–51.
- Kasuya A, Hamaguchi Y, Fujimoto M, et al. TIF1 $\gamma$ -overexpressing, highly progressive endometrial carcinoma in a patient with dermatomyositis positive for malignancy-associated anti-p155/140 autoantibody. *Acta Derm Venereol* 2013;93:715–6.
- Pinal-Fernandez I, Ferrer-Fabregas B, Trallero-Araguás E, et al. Tumour TIF1 mutations and loss of heterozygosity related to cancer-associated myositis. *Rheumatology* 2018;57:388–96.
- Mohassel P, Rosen P, Casciola-Rosen L, et al. Expression of the dermatomyositis autoantigen transcription intermediary factor 1 $\gamma$  in regenerating muscle. *Arthritis Rheumatol* 2015;67:266–72.
- Oya K, Inoue S, Saito A. Pregnancy triggers the onset of anti-transcriptional intermediary factor 1 $\gamma$  antibody-positive dermatomyositis: a case series. *Rheumatology* 2019.
- Yan K-P, Dollé P, Mark M, et al. Molecular cloning, genomic structure, and expression analysis of the mouse transcriptional intermediary factor 1 gamma gene. *Gene* 2004;334:3–13.
- Hesling C, Lopez J, Fattet L, et al. Tif1 $\gamma$  is essential for the terminal differentiation of mammary alveolar epithelial cells and for lactation through Smad4 inhibition. *Development* 2013;140:167–75.
- Müller U, Steinhoff U, Reis LF, et al. Functional role of type I and type II interferons in antiviral defense. *Science* 1994;264:1918–21.
- Sugihara T, Sekine C, Nakae T, et al. A new murine model to define the critical pathologic and therapeutic mediators of polymyositis. *Arthritis Rheum* 2007;56:1304–14.
- Okiyama N, Sugihara T, Oida T, et al. T lymphocytes and muscle condition act like seeds and soil in a murine polymyositis model. *Arthritis Rheum* 2012;64:3741–9.
- Okiyama N, Furumoto Y, Villarroel VA, et al. Reversal of CD8 T-cell-mediated mucocutaneous graft-versus-host-like disease by the JAK inhibitor tofacitinib. *J Invest Dermatol* 2014;134:992–1000.
- Nagaraju K, Plotz PH. Animal models of myositis. *Rheum Dis Clin North Am* 2002;28:917–33.
- Ascherman DP. Animal models of inflammatory myopathy. *Curr Rheumatol Rep* 2012;14:257–63.
- Rosenberg NL, Ringel SP, Kotzin BL. Experimental autoimmune myositis in SJL/J mice. *Clin Exp Immunol* 1987;68:117–29.
- Matsubara S, Shima T, Takamori M. Experimental allergic myositis in SJL/J mice immunized with rabbit myosin B fraction: immunohistochemical analysis and transfer. *Acta Neuropathol* 1993;85:138–44.
- Okiyama N, Sugihara T, Iwakura Y, et al. Therapeutic effects of interleukin-6 blockade in a murine model of polymyositis that does not require interleukin-17A. *Arthritis Rheum* 2009;60:2505–12.
- Katsumata Y, Ridgway WM, Oriss T, et al. Species-specific immune responses generated by histidyl-tRNA synthetase immunization are associated with muscle and lung inflammation. *J Autoimmun* 2007;29:174–86.
- Sgroi D, Cohen RN, Lingenheld EG, et al. T cell lines derived from the spinal cords of mice with experimental allergic encephalomyelitis are self reactive. *J Immunol* 1986;137:1850–4.
- Nagaraju K, Raben N, Villalba ML, et al. Costimulatory markers in muscle of patients with idiopathic inflammatory myopathies and in cultured muscle cells. *Clin Immunol* 1999;92:161–9.
- Bartocioni E, Gallucci S, Scuderi F, et al. Mhc class I, MHC class II and intercellular adhesion molecule-1 (ICAM-1) expression in inflammatory myopathies. *Clin Exp Immunol* 1994;95:166–72.
- Nagaraju K, Casciola-Rosen L, Lundberg I, et al. Activation of the endoplasmic reticulum stress response in autoimmune myositis: potential role in muscle fiber damage and dysfunction. *Arthritis Rheum* 2005;52:1824–35.
- Arahata K, Engel AG. Monoclonal antibody analysis of mononuclear cells in myopathies. V: identification and quantitation of T8+ cytotoxic and T8+ suppressor cells. *Ann Neurol* 1988;23:493–9.
- Dalakas MC, Hohlfeld R. Polymyositis and dermatomyositis. *Lancet* 2003;362:971–82.
- Nagaraju K, Raben N, Loeffler L, et al. Conditional up-regulation of MHC class I in skeletal muscle leads to self-sustaining autoimmune myositis and myositis-specific autoantibodies. *Proc Natl Acad Sci U S A* 2000;97:9209–14.
- Shimizu K, Kobayashi T, Kano M, et al. Anti-transcriptional intermediary factor 1- $\gamma$  antibody as a biomarker in patients with dermatomyositis. *J Dermatol* 2020;47:64–8.
- Ceribelli A, Isailovic N, De Santis M, et al. Myositis-specific autoantibodies and their association with malignancy in Italian patients with polymyositis and dermatomyositis. *Clin Rheumatol* 2017;36:469–75.
- Ikeda N, Yamaguchi Y, Kanaoka M, et al. Clinical significance of serum levels of anti-transcriptional intermediary factor 1- $\gamma$  antibody in patients with dermatomyositis. *J Dermatol* 2020;47:490–6.
- Bergua C, Chiavelli H, Allenbach Y, et al. In vivo pathogenicity of IgG from patients with anti-SRP or anti-HMGCR autoantibodies in immune-mediated necrotising myopathy. *Ann Rheum Dis* 2019;78:131–9.
- Uruha A, Nishikawa A, Tsuburaya RS, et al. Sarcoplasmic MxA expression: a valuable marker of dermatomyositis. *Neurology* 2017;88:493–500.
- Okiyama N, Yamaguchi Y, Kodera M, et al. Distinct histopathologic patterns of finger eruptions in dermatomyositis based on myositis-specific autoantibody profiles. *JAMA Dermatol* 2019. doi:10.1001/jamadermatol.2019.1668. [Epub ahead of print: 10 Jul 2019].
- Hornung T, Janzen V, Heidgen F-J, et al. Remission of recalcitrant dermatomyositis treated with ruxolitinib. *N Engl J Med* 2014;371:2537–8.
- Ladislau L, Suárez-Calvet X, Toquet S, et al. Jak inhibitor improves type I interferon induced damage: proof of concept in dermatomyositis. *Brain* 2018;141:1609–21.
- Aeschlimann FA, Frémond M-L, Duffy D, et al. A child with severe juvenile dermatomyositis treated with ruxolitinib. *Brain* 2018;141:e80.
- Paik JJ, Christopher-Stine L. A case of refractory dermatomyositis responsive to tofacitinib. *Semin Arthritis Rheum* 2017;46:e19.



## Supplemental Materials and Methods

### Recombinant human TIF1 $\gamma$ protein.

A full-length human TIF1 $\gamma$  gene (GenBank accession Number: AF119043) was His-tagged at its 3' end and inserted into pFastBac1 vector for baculovirus expression (Invitrogen). Recombinant bacmids produced using the expression vectors were transfected into SF9 cells using Cellfectin II (Invitrogen). The infected SF9 cells were incubated for 48 hours at 27 °C and then harvested and lysed by sonication. The soluble cell lysate from  $8 - 10 \times 10^7$  cells/15 ml was applied onto a Ni Sepharose 6 Fast Flow Resin column (GE Healthcare). The purified recombinant protein was collected from 2<sup>nd</sup> and 3<sup>rd</sup> fractions eluted with phosphate buffer containing 200 mM imidazole, and concentrated to  $> 1$  mg/ml using Centriprep<sup>®</sup> Centrifugal Filter Devices YM-50 (Millipore).

### Histological scoring system for experimental myositis

The histological severity of inflammation in each muscle block of the hamstrings and quadriceps was graded as follows: grade 1 = involvement of 1-4 muscle fibers; grade 2 = a lesion involving 5-30 muscle fibers; grade 3 = a lesion involving a muscle fasciculus; and grade 4 = diffuse and extensive lesions. When multiple lesions with the same grade were found in a single muscle block, 0.5 point was added to the grade. The histological severity in each mouse was determined as the average of the hamstring and quadriceps blocks.

**Generation of antigen-pulsed mature bone marrow–derived dendritic cells****(BMDCs).**

BMDCs were generated from BM cells of B6 mice cultured in RPMI1640 with 10% fetal bovine serum (FBS) and 20 ng/ml recombinant murine granulocyte-macrophage colony stimulating factor (Wako Junyaku) for 8 days. The cells were incubated with 50 µg/ml of the recombinant TIF1γ protein and 1 µg/ml lipopolysaccharide (Sigma-Aldrich) for an additional 24 hours. More than 70% of the treated cells were CD11c-positive.

**Cell proliferation assay.**

T cells were purified from the inguinal and popliteal lymph node (LN) cells of immunized mice 14 days after the last immunization using CD3 T cell enrichment columns (R&D systems). Two hundred thousand T cells and  $2 \times 10^4$  mature BMDCs were cultured in 200 µl RPMI1640 with 10% FBS for 3 days using 96-well round-bottom plates, into which 1 µCi [<sup>3</sup>H]thymidine was added during the last 18 hours of culture. Proliferation of the T cells was evaluated as radioactivity of harvested cells counted by a β counter (MicroBeta™, Perkin Elmer).

**Enzyme-linked immunosorbent assay (ELISA).**

The plasma samples collected from immunized mice 2 weeks after the last immunization were diluted at 1:100 or 1:1000 and then incubated in 96-well flat-bottom microtiter plates, which had been coated with 3 ng/ml of full-length human TIF1γ for 1 hour at 37 °C. Pooled plasma from three TIF1γ-immunized mice was used as the positive control and plasma from one CFA-treated mouse was the negative control.

Plates were washed four times then incubated with peroxidase-conjugated goat anti-murine IgG antibodies (ab205719, Abcam) and visualized by incubation with 3, 3', 5, 5'-tetramethyl-benzidine for 1 hour at room temperature. The reactions were stopped by 0.5 N sulfuric acid. Optical density (OD) at 450 nm was measured, and each antibody index was calculated from the formula:  $([\text{sample OD} - \text{blank OD}] / [\text{positive reference OD} - \text{blank OD}]) \times 100$ .

### **Immunohistochemical analyses (IHC)**

Sections (6  $\mu\text{m}$ ) from formalin-fixed paraffin-embedded muscle tissue samples were pretreated with Trilogy<sup>TM</sup> (Merck), and stained with rabbit anti-mouse CD8 $\alpha$  (EPR20305; Abcam), rabbit anti-mouse CD4 (EPR19514; Abcam), and rat anti-mouse/human B220 (RA3-6B2; BD Biosciences PharMingen) monoclonal antibodies, and rabbit anti-rat/human/mouse CD11b polyclonal antibodies (product number, PA5-79533, Invitrogen). Nonspecific staining was blocked with 5-10% bovine serum albumin (BSA). Bound antibodies were visualized with peroxidase-labeled anti-rabbit/mouse IgG antibody (Envision<sup>TM</sup>+ Dual Link System-HRP; Dako) or goat anti-rat IgG antibody (Abcam), and associated substrates (Liquid DAB+ Substrate Chromogen System; Dako). Cryostat-frozen sections (6  $\mu\text{m}$ ) fixed in cold acetone were preincubated with 5% BSA, stained with mouse anti-mouse H-2K<sup>b</sup> monoclonal antibody (AF6-88.5; BioLegend), and visualized with peroxidase-labeled goat anti-mouse/rabbit IgG antibodies and its substrates (Dako). Isotype controls were used as negative control. The stained sections were evaluated by two independent observers, who reported results that were comparable.

### ***In vivo* depletion of CD8<sup>+</sup> T cells**

Mice were injected intraperitoneally with 1 mg of purified rat anti-CD8 $\alpha$  depleting monoclonal antibody (53.67.2), produced by hybridoma cells cultured in CELLLine flasks (WHEATON) with Hybridoma-SFM (Gibco), or purified rat IgG2b (BioXCell) as a control, for three consecutive days. This treatment started 10 days before the 4<sup>th</sup> immunization, and injection of 500  $\mu$  of the same antibody was repeated every other day for 14 days. Complete depletion of CD8<sup>+</sup> T cells in the splenocytes were confirmed by flow cytometric analysis.

### **Real-time quantitative polymerase chain reaction (RT-qPCR) analyses**

Total RNA was extracted from the muscle tissue samples using Trizol Reagent (Invitrogen). Complementary DNA was synthesized with a High-Capacity cDNA Reverse Transcription Kit (Thermo Fisher). Levels of expression were detected using the QuantStudio™ 5 Real-Time PCR Systems (Applied Biosystems) with PrimeTime® Gene Expression Master Mix and Prime Time qPCR predesigned primers (Integrated DNA Technologies; Supplemental Table 1). All RT-qPCR analyses were performed in triplicate. Amplification products were quantified by the comparative CT method. The mRNA level of each gene was normalized to that of Actb.

**Supplemental Table 1. Primers for real-time quantitative polymerase chain reactions**

Target	ID
<i>Mxl</i>	Mm.PT.58.12101853.g
<i>Isg15</i>	Mm.PT.58.41476392.g
<i>Osa1b</i>	Mm.PT.56 $\alpha$ .10289138.g
<i>Osa3</i>	Mm.PT.58.12139602